

# Analytical Modeling the Substrate Effect in Symmetric Coupled Interconnects of High-Speed VLSI Circuits

H. Ymeri<sup>a\*</sup>, B. Nauwelaers<sup>a</sup>, Karen Maex<sup>a,b</sup>, D. De Roest<sup>b</sup>

<sup>a</sup>*Katholieke Universiteit Leuven, Department of Electrical Engineering (ESAT),*

*Division ESAT-TELEMIC, Kasteelpark Arenberg 10, B-3001 Leuven-Heverlee, Belgium*

<sup>b</sup>*The Interuniversity Microelectronics Center (IMEC), Kapeldreef 75, B-3001 Leuven, Belgium*

Recebido em 23 de Junho, 2003.

New analytical approximations for the frequency-dependent impedance matrix components of symmetric VLSI interconnect on lossy silicon substrate are derived. The results have been obtained by using an approximate quasi-magnetostatic analysis of symmetric coupled microstrip on-chip interconnects on silicon. We assume that the magnetostatic field meets the boundary conditions of a single isolated infinite line; therefore the boundary conditions for the conductors in the structure are approximately satisfied. The derivation is based on the approximate solution of quasi-magnetostatic equations in the structure (dielectric and silicon semi-space), and takes into account the substrate skin effect. Comparisons with published data from circuit modeling or full-wave numerical analyses are presented to validate the inductance and resistance expressions derived for symmetric coupled VLSI interconnects. The analytical characterization presented in the paper is well situated for inclusion into CAD codes in the design of RF and mixed-signal integrated circuits on silicon.

Key words: VLSI interconnect, quasi-magnetostatic analysis, distributed Inductance and resistance, silicon substrate, analytical approximation.

## 1 Introduction

With high clock frequencies and faster transistor rise/fall time in modern VLSI circuits, long signal wires exhibit transmission line effects. As a consequence, the electrical characteristics of the interconnections are becoming important factors in the behavior of VLSI circuits. Hence, they must be known with greater accuracy in order to avoid the necessity of using large safety margins leading to sub-optimal designs. Therefore, the traditional methods of parasitic extraction are no longer adequate. Much improved procedures will be necessary to generate electrical models for the interconnections that accurately account for such effects as delay, crosstalk, substrate skin-effect, resistive voltage drops, etc. These new methods must be simple, quick, accurate, efficient, flexible and CAD-oriented.

Currently, the most commonly used substrate material for VLSI circuits is silicon, and depending on its doping rate, the conductivity can vary over more than four decades, e. g. from 1 S/m to  $10^5$  S/m. The broad-band transmission line behavior of interconnects on lossy silicon substrate has been characterized by experiments [1 - 4], by rigorous semi-analytical methods, and by various full-wave numerical procedures [5 - 10].

In recent works [11 - 14], the authors succeeded to describe the frequency-dependent series impedance matrix

components of generally asymmetric coupled on-chip interconnects on lossy silicon substrate in a unified way. Therefore, the influence of the conducting substrate is expressed by closed-form frequency-dependent inductance and resistance per unit length parameters. The extent to which the conducting substrate affects the performance of an integrated circuit depends not only on the conductivity of the silicon and the frequency but also on the geometry (width, thickness, distance to adjacent lines and to the substrate, etc) as well as on the material of the interconnects (usually Al or Cu).

The purpose of the present paper is to develop CAD-oriented, analytical approximations for the frequency-dependent series impedance matrix components of general, symmetric coupled on-chip interconnects on silicon substrate. The proposed model includes the important physical effects (substrate skin-effect) associated with on-chip interconnects on silicon. In this work, a general quasi-magnetostatic analysis based on quasi-TEM assumption is applied to compute the frequency-dependent distributed resistance and inductance parameters. The following derivation assumes that the electric and magnetic fields meet the boundary conditions of a single isolated infinite wire. It will be demonstrated by the full-wave solver that for a class of typical on-chip interconnects on silicon substrate with small conductor cross sections, the frequency-dependent behavior

\*Corresponding author. Tel.: + 32-16-321-876; Fax: + 32-16-321-986. E-mail address: Hasan.Ymeri@esat.kuleuven.ac.be (H. Ymeri).

of the series impedance matrix component parameters may be dominated by the substrate skin-effect. Because of the very small cross sections of on-chip interconnects, the skin effect inside the lines can mostly be neglected up to very high frequencies (e. g. 20 GHz and more). Finally, the results were obtained by applying these simple and accurate expressions will be compared to results gained from very accurate full-wave solvers and CAD-oriented circuit modeling approach.

## 2 Quasi-magnetostatic analysis of symmetric interconnects on silicon

Interconnect models must incorporate distributed transmission line matrices  $[R]$ ,  $[L]$ ,  $[G]$ , and  $[C]$  to accurately estimate interconnect delay and cross-talk in a multilevel network for multi-GHz gigascale integration (GSI).

To determine the frequency-dependent resistance and inductance matrices components of interconnects on lossy silicon, a quasi-TEM mode formulation is applied. When assuming a quasi-TEM mode of wave propagation, an electro- and magneto-static analysis can be used to determine the transverse electric and magnetic fields of an interconnect structure; therefore the reduced set of the Maxwell's equations is

$$\nabla \times \mathbf{H} = \mathbf{J} \quad (1)$$

$$\nabla \circ \mathbf{B} = 0 \quad (2)$$

and

$$\mathbf{B} = \mu \mathbf{H} \quad (3)$$

where  $\mathbf{H}$  is the vector of the magnetic field intensity,  $\mathbf{B}$  is the vector of the magnetic flux density,  $\mathbf{J}$  is the vector of the current density, and  $\mu$  is the magnetic permeability.

For quasi-magnetostatics, let the vector potential be  $\mathbf{A}$  such that

$$\mathbf{B} = \nabla \times \mathbf{A}. \quad (4)$$

Combining Eqs. (1), (3) and (4), we can show that the inductive electric equals field is given by

$$\mathbf{E} = -\frac{\partial \mathbf{A}}{\partial t}. \quad (5)$$

To develop an expression for the series per-unit length impedance matrix  $[Z]$  of a symmetric coupled on-chip interconnects on lossy silicon substrate, as illustrated in Fig. 1a, the given structure can be regarded as a system of inductively coupled transmission lines with the silicon substrate acting as the return line. Results obtained from the full-wave analysis [6, 11 - 14] have shown that the influence of the finite substrate thickness  $t_{si}$  can be neglected for practical dimensions (i.e.,  $t_{si} \gg w$ ,  $t_{si} \gg t_m$ ,  $t_{si} \gg s$ , and  $t_{si} \gg t_{ox}$ ). The silicon substrate is therefore assumed to be

infinitely thick in the following modeling approach (see Fig. 1b).

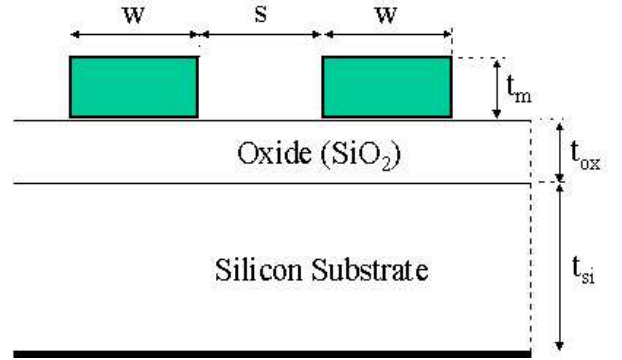


Figure 1(a). Cross section of symmetric coupled interconnects on an oxide-semiconductor substrate.

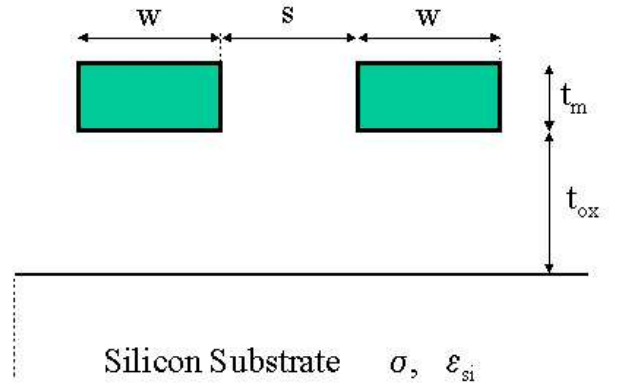


Figure 1(b). Symmetric coupled interconnect lines over infinite thick silicon substrate.

For the case of a symmetric coupled interconnect lines with lossy conductors and lossy silicon substrate, the series per unit length impedance matrix  $[Z]$  can be written as

$$[Z] = j\omega[L] + [Z_w(\omega)] + [Z_{si}(\omega)] \quad (6)$$

where  $[Z_w]$  and  $[Z_{si}]$  are the wire (interconnect) and the silicon substrate impedance per unit length matrices, respectively, and  $[L]$  is the external per unit length inductance matrix calculated for a lossless interconnects above a perfectly conducting silicon substrate.

### 2.1 External inductance matrix calculation

The external inductance matrix components are calculated from the magnetic flux density in the regions surrounding the interconnect conductors. As a first step, round-sectioned lines embedded in an electrically homogeneous medium are assumed, which is realistic for most microelectronic micrometre designs. This was found permissible (see numerical results) and simplifies the analysis considerably. The real and equivalent structures are shown in Fig. 2, where the rectangular to circular conversion is used.

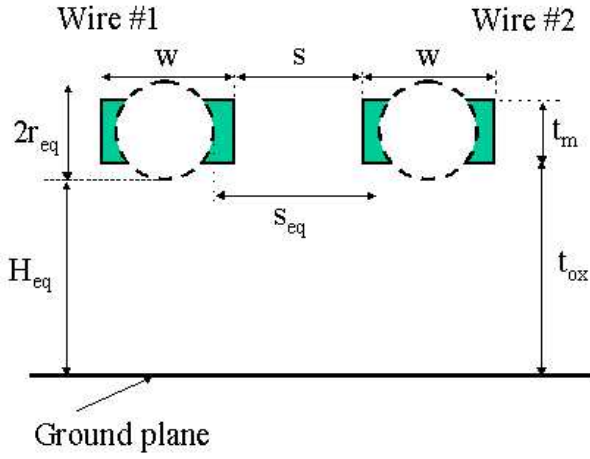


Figure 2. Equivalent circular-sectioned interconnect lines over perfectly conducting ground plane (top surface of silicon).

To model actual rectangular conductors, we define an equivalent diameter  $2r_{eq}$  as the mean of the diameters of the two circles inscribed in the conductors, e.g.

$$2r_{eq} = \frac{w + t_m}{2}. \quad (7)$$

The other geometrical dimensions  $t_{ox}$  and  $s$  are consequently redefined as

$$H_{eq} = t_{ox} + \frac{t_m - w}{4}, \quad (8)$$

$$s_{eq} = s + \frac{w - t_m}{4} + \frac{w - t_m}{4}. \quad (9)$$

The total flux linkage of each conductor (labeled one and two in Fig. 2) is calculated using the inductance matrix given by

$$\begin{bmatrix} \Phi_1 \\ \Phi_2 \end{bmatrix} = \begin{bmatrix} L_{11} & L_{12} \\ L_{21} & L_{22} \end{bmatrix} \begin{bmatrix} I_1 \\ I_2 \end{bmatrix}, \quad (10)$$

where  $\Phi_1$  and  $\Phi_2$  are the flux linkages per unit length of each conductor,  $I_1$  and  $I_2$  are the currents through each conductor,  $L_{11}$  and  $L_{22}$  are the self-inductances per unit length of each conductor, and  $L_{12}$  and  $L_{21}$  are the mutual inductance per unit length between conductors. Because each wire in Fig. 2 has an identical geometrical configuration (symmetric interconnect lines), then

$$L_s = L_{11} = L_{22} \quad (11)$$

$$L_m = L_{12} = L_{21}. \quad (12)$$

To calculate the self- and mutual inductances for this configuration, wire one is excited by a constant current source  $I$  and wire two has zero current. Using (10) the resulting expressions for the self- and mutual inductances are given by

$$L_s = \frac{\Phi_1}{I} \quad (13)$$

and

$$L_m = \frac{\Phi_2}{I}. \quad (14)$$

As seen in Fig. 3 the flux linkage per unit length for each conductor is determined by calculating the total flux through surface one ( $\Phi_1$ ) for the self-inductance and the total flux through surface two ( $\Phi_2$ ) for the mutual inductance.

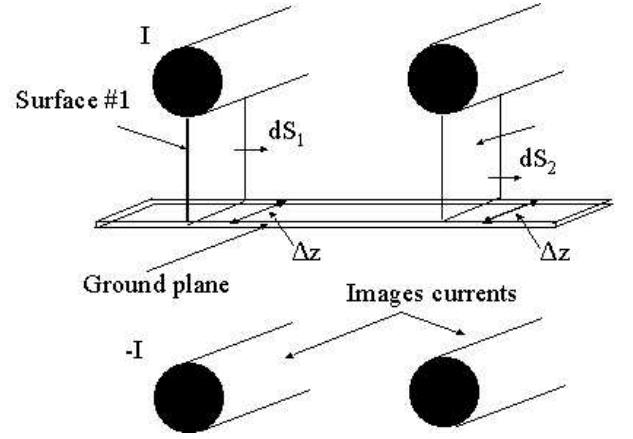


Figure 3. Method of images and mutual and self flux for line one.

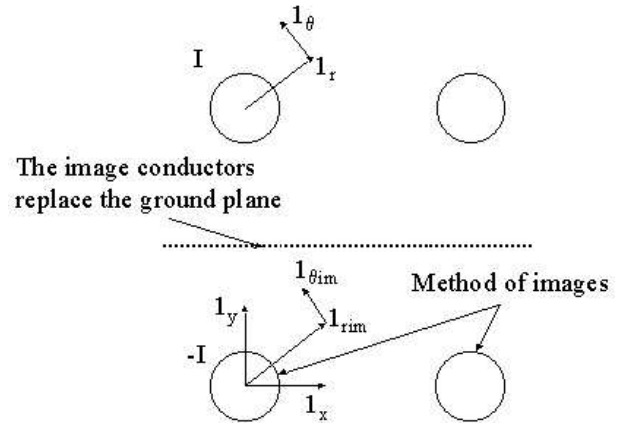


Figure 4. Coordinate system for calculating magnetic fields.

To calculate the magnetic fields above an infinite ground plane (top silicon surface) the method of images is used. As seen in Fig. 3 the image line one replaces the ground plane such that the current in the image line is in the opposite direction of the current in line one. It is assumed that each of these lines produces magnetic fields as they would if they were each isolated from each other (therefore the boundary conditions for the conductors in the configuration are approximately satisfied with this isolated line assumption). Therefore the magnetic fields are given by the following relationships using the two coordinate systems in Fig. 4

$$\mathbf{B}_1 = \frac{\mu I}{2\pi r} \mathbf{1}_\theta \quad (15)$$

$$\mathbf{B}_{1im} = -\frac{\mu I}{2\pi r_{im}} \mathbf{1}_{\theta_{im}} \quad (16)$$

where the sub-index  $im$  denote the coordinates of the image current source. The total flux linkage for line 1 is given by the surface integral of a surface connecting line 1 to the ground as seen in Fig. 3. Assuming that the magnetic fields

$$\Phi_1 = \int_{y=h}^{y=2h-r_{eq}} \left\{ \frac{\mu I}{2\pi r} \mathbf{1}_\theta \circ \mathbf{1}_x dy \Delta z - \frac{\mu I}{2\pi r_{im}} \mathbf{1}_{\theta im} \circ \mathbf{1}_x dy \Delta z \right\}. \quad (17)$$

The introduction of  $\Delta z$  has enabled the surface integral in Fig. 3 to be transformed into a line integral. Because three coordinate systems are involved in Fig. 4, the dot product between the unit vectors in each coordinate system must be resolved. From inspection of Fig. 4, the results are

$$\mathbf{1}_\theta \circ \mathbf{1}_x = 1 \quad (18)$$

and

$$\mathbf{1}_{\theta im} \circ \mathbf{1}_x = -1. \quad (19)$$

Making these substitutions into (17), we get

$$\Phi_1 = \frac{\mu I \Delta z}{2\pi} \int_{y=h}^{y=2h-r_{eq}} \left\{ \frac{dy}{2h-y} + \frac{dy}{y} \right\} = \frac{\mu I \Delta z}{2\pi} [-\ln(2h-y) + \ln y] \Big|_{y=h}^{y=2h-r_{eq}}. \quad (23)$$

Evaluating (23) gives

$$\Phi_1 = \frac{\mu I \Delta z}{2\pi} \left[ \ln \left( \frac{y}{2h-y} \right) \Big|_{y=h}^{y=2h-r_{eq}} \right] = \frac{\mu I \Delta z}{2\pi} \left\{ \ln \left[ \frac{2h-r_{eq}}{2h-2h+r_{eq}} - \ln \left( \frac{h}{2h-h} \right) \right] \right\}. \quad (24)$$

The final expression for the flux linkage per unit length is

$$\frac{\Phi_1}{\Delta z} = \frac{\mu I}{2\pi} \left[ \ln \left( \frac{2H_{eq} + r_{eq}}{r_{eq}} \right) \right]. \quad (25)$$

The self-inductance per unit length is then define from (13) to be

$$L_{11} = \frac{\Phi_1}{I \Delta z} = \frac{\mu}{2\pi} \left[ \ln \left( \frac{2H_{eq} + r_{eq}}{r_{eq}} \right) \right]. \quad (26)$$

of each line superimpose, the flux linkage for line 1 is determined from the line integral starting at the edge of the ground plane ( $y = h = H_{eq} + r_{eq}$ ) and ending at the edge of the real conductor ( $y = 2h - r_{eq}$ ) and is given by

$$\Phi_1 = \int_{y=h}^{y=2h-r_{eq}} \left\{ \frac{\mu I}{2\pi r} dy \Delta z + \frac{\mu I}{2\pi r_{im}} dy \Delta z \right\}. \quad (20)$$

Finally, the relationship between the variables in three various coordinate systems along the above integral must be determined. From inspection of Fig. 4, the relationships are

$$r = 2h - y \quad (21)$$

$$r_{im} = y. \quad (22)$$

making these substitution into (20) gives

The mutual flux is the amount of flux linkages of surface no. 2 from a current in conductor 1. The flux linkages of surface no. 2 are calculated by a surface connecting conductor 2 and the ground plane. Using the superimposed magnetic fields and the coordinate system in Fig. 5 gives the following expression for the flux linking line 2 to the ground plane in surface 2 as

$$\Phi_2 = \int_{y=h}^{y=2h-r_{eq}} \left\{ \frac{\mu I}{2\pi r} \mathbf{1}_\theta \circ \mathbf{1}_x dy \Delta z - \frac{\mu I}{2\pi r_{im}} \mathbf{1}_{\theta im} \circ \mathbf{1}_x dy \Delta z \right\}. \quad (27)$$

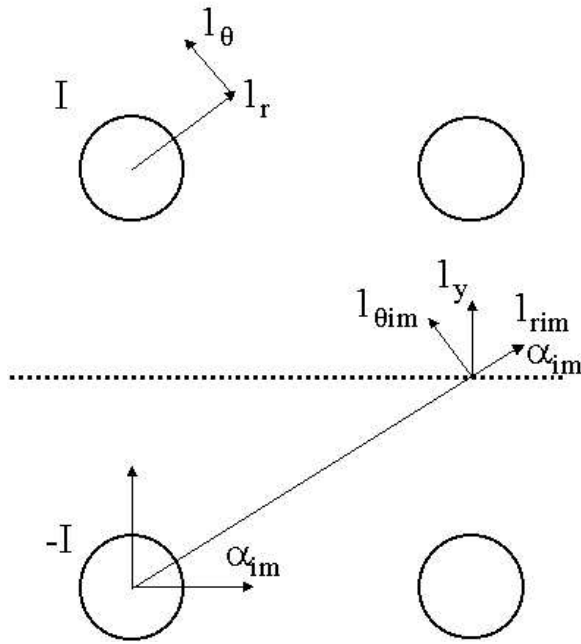


Figure 5. Coordinate system for calculating magnetic fields.

Because three coordinate systems are involved in Fig. 5, the dot product between the unit vectors in each coordinate system must be calculated. From inspection of Fig. 5, the results are

$$\mathbf{l}_\theta \circ \mathbf{l}_x = \cos(90 - \alpha) = \sin \alpha = \frac{2h - y}{r} \quad (28)$$

$$\mathbf{l}_{\theta im} \circ \mathbf{l}_x = \cos(90 + \alpha) = -\sin \alpha = -\frac{y}{r_{im}}. \quad (29)$$

Making these substitution in (27) gives

$$\Phi_2 = \frac{\mu I}{2\pi} \Delta z \int_{y=h}^{y=2h-r_{eq}} \left\{ \frac{(2h-y)dy}{r^2} + \frac{ydy}{r_{im}^2} \right\}. \quad (30)$$

Finally, the relationship between the variables in the various coordinate systems along the above integral must be determined. From inspection of Fig. 5, the following relationships must hold

$$r^2 = d^2 + (y - 2h)^2, \quad (31)$$

$$r_{im}^2 = d^2 + y^2, \quad (32)$$

where  $d = s_{eq} + 2r_{eq}$ . Making these substitutions into (30) gives

$$\begin{aligned} \Phi_2 &= \frac{\mu I}{2\pi} \Delta z \int_{y=h}^{y=2h-r_{eq}} \left\{ -\frac{(y-2h)dy}{d^2 + (y-2h)^2} + \frac{ydy}{d^2 + y^2} \right\} \\ &= \frac{\mu I}{2\pi} \Delta z \left\{ -\frac{1}{2} \ln [d^2 + (y-2h)^2] + \ln(d^2 + y^2) \right\} \Bigg|_{y=h}^{y=2h-r_{eq}}. \end{aligned} \quad (33)$$

Evaluating (33), we get

$$\begin{aligned} \frac{\Phi_2}{\Delta z} &= \frac{\mu I}{2\pi} \left[ \ln \sqrt{\frac{d^2 + y^2}{d^2 + (y-2h)^2}} \right] \Bigg|_{y=h}^{y=2h-r_{eq}} \\ &= \frac{\mu I}{2\pi} \left[ \ln \sqrt{\frac{d^2 + (2h-r_{eq})^2}{d^2 + r_{eq}^2}} - \ln \sqrt{\frac{d^2 + h^2}{d^2 + (h-2h)^2}} \right]. \end{aligned} \quad (34)$$

The final expression for the flux linkage per unit length for line 2 is

$$\frac{\Phi_2}{\Delta z} = \frac{\mu I}{2\pi} \left[ \ln \sqrt{\frac{d^2 + (2h-r_{eq})^2}{d^2 + (r_{eq})^2}} \right]. \quad (35)$$

The mutual inductance per unit length is defined from (14) to be

$$L_{12} = \frac{\Phi_2}{I \Delta z} = \frac{\mu}{2\pi} \left[ \ln \sqrt{\frac{d^2 + (2h-r_{eq})^2}{d^2 + (r_{eq})^2}} \right]. \quad (36)$$

The approximate closed-form expressions for the self and mutual inductance per unit length are given by

$$L_s = \frac{\mu}{2\pi} \ln \left[ \frac{2H_{eq} + r_{eq}}{r_{eq}} \right] \quad (36)$$

and

$$L_m = \frac{\mu}{2\pi} \ln \sqrt{\frac{(s_{eq} + 2r_{eq})^2 + (2H_{eq} + r_{eq})^2}{(s_{eq} + 2r_{eq})^2 + (r_{eq})^2}}. \quad (37)$$

## 2.2 Silicon substrate impedance per unit length calculation

The problem of propagation along a transmission line composed of a single interconnect on a lossy silicon substrate was treated by H. Ymeri et al. [11 - 14]. Recently, several other authors have dealt with the same problem (e.g. [2, 4, 5, 15]). The series impedance per unit length of lossy silicon can be viewed as a correction factor to the interconnect line series impedance per unit length when the silicon substrate is not a perfect conductor and it can be defined as

$$Z_{si} = \frac{j\omega \int_{-\infty}^{t_{ox}} \mu H_x^{sc}(y, z) dz}{I} - j\omega L_s \quad (38)$$

where  $L_s$  is the inductance per unit length of the interconnect conductor calculated for a lossless interconnect strip above a perfectly conducting silicon substrate (see expression (36)), and  $H_x^{sc}(y, z)$  is the x-component of the scattered magnetic field. Little generality is lost by considering this quasi-TEM case, and so only the z component of the

current, and thus the x component of the H-field is needed [16].

Neglecting the vertical component of the scattered H-field inside the lossy silicon substrate, the following expression for the internal silicon substrate impedance per unit length  $Z_{si}$  can be derived (see for instance [17])

$$Z_{si} = \frac{j\omega\mu}{\pi} \int_0^\infty \frac{e^{-2t_{ox}z}}{\sqrt{z^2 + \gamma_{si}^2} + z} dz \quad (39)$$

where  $\gamma_{si}$  is the propagation constant in the lossy silicon substrate given by

$$\gamma_{si} = \sqrt{j\omega\mu(\sigma_{si} + j\omega\epsilon_{rsi}\epsilon_0)} \quad (40)$$

and  $\sigma_{si}$ ,  $\epsilon_{rsi}$  are the silicon conductivity and relative permittivity, respectively.

It is possible to express (40) in an equivalent form involving the modified Bessel function of the second kind, written as

$$K_1(\mathbf{m}) = \mathbf{m} \int_1^\infty \sqrt{z^2 - 1} e^{-\mathbf{m}z} dz \quad (41)$$

where  $\mathbf{m}$  is a complex argument. Using (41) and after some straightforward mathematical manipulations, the internal impedance per unit length of silicon substrate can be written in the following equivalent form

$$Z_{si} = \frac{j\omega\mu}{2\pi} \left\{ \frac{2}{\mathbf{n}^2} + 2j \int_0^1 (\sqrt{1-z^2}) e^{-\mathbf{n}z} dz - \frac{2K_1(\mathbf{n})}{\mathbf{n}} \right\} \quad (42)$$

in which  $\mathbf{n} = 2\gamma_{si}t_{ox}$ .

It can be seen that the silicon impedance per unit length depends considerably on both silicon conductivity and the interconnect strip height above silicon surface. On the other hand, the influence of the silicon relative permittivity appears only for frequencies higher than some few GHz.

According to the method presented and discussed by Ymeri et al [11 - 14], and the methodology used in [17], at the same time leaving out the details, it can be shown that the approximate closed-form expressions for internal silicon impedance per unit length components can be written in the form:

$$Z_{siii} = \frac{j\omega\mu}{2\pi} \log \left( \frac{1 + \gamma_{si}t_{ox}}{\gamma_{si}t_{ox}} \right). \quad (43)$$

$$Z_{sijj} = \frac{j\omega\mu_0}{4\pi} \log \left\{ \frac{(1 + \gamma_{si}t_{ox})^2 + \left(\frac{\gamma_{si}s}{2}\right)^2}{(\gamma_{si}t_{ox})^2 + \left(\frac{\gamma_{si}s}{2}\right)^2} \right\}. \quad (44)$$

## 3 Discussion of the results

The proposed analytic expressions for series resistance and inductance per unit length have been applied to various on-chip interconnects on lossy silicon substrate. To illustrate the accuracy of the proposed modeling approach, the frequency-dependent self and mutual resistance and inductance parameters for a coupled on-chip interconnect structure on a low resistivity ( $\rho_{si} = 0.01 \Omega\text{cm}$ ) silicon substrate of  $300 \mu\text{m}$  thickness have been computed using our procedure, and compared with the solution obtained by the quasi-magnetostatic analysis and full-wave solutions. The cross section of each conductor is  $2 \mu\text{m} \times 1 \mu\text{m}$  and the separation between the conductors is  $2 \mu\text{m}$ . The thickness of an oxide layer is  $2 \mu\text{m}$ . For the case of highly conductive silicon substrate, the skin effect plays an important role in the current distribution at high frequencies, and forces the return current to the surface of the silicon as the frequency increases. As a result, at high frequencies, the return current in the silicon closely matches the current carried by the signal conductor. Figs. 6 and 7 show the frequency-dependent impedance matrix parameters for symmetric coupled interconnects on lossy silicon substrate. As expected, the highly

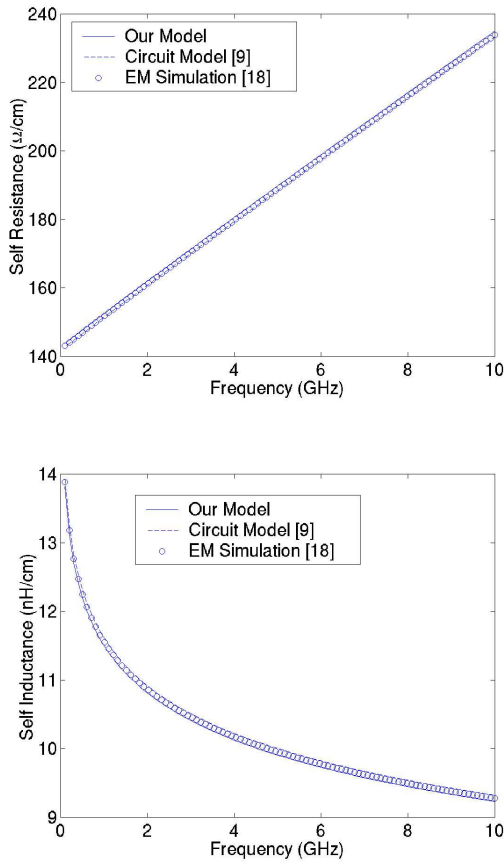


Figure 6. Self impedance parameters for symmetric coupled interconnects on low-resistivity silicon substrate. (a) Self resistance as a function of frequency, and (b) Self inductance as a function of frequency.

conductive silicon has more significant impact on the frequency-dependence of the line parameters as compared to the medium-resistivity silicon. In the case of medium and high resistivity silicon substrate, however, the substrate skin effect is seen to be negligible. For medium or high substrate resistivity, the distributed inductance can be computed directly from the distributed capacitance  $C_{air}$  obtained with all dielectrics removed. In this case, the expression for the inductance calculation  $L = \mu_0 \epsilon_0 C_{air}^{-1}$  can be used. For low-resistivity silicon substrate, there is for current signal frequencies a considerable skin-effect in the substrate, and, consequently, the inductive coupling becomes frequency dependent (the higher the frequencies the smaller the self and mutual inductances). The coupling effects depend on the interconnect lines geometry, especially on the distance of the lines from the substrate. Another important effect is frequency-dependent losses resulting from the skin effect in the silicon. On account of the very small cross-sections of on-chip interconnects, the skin effect inside the signal lines can mostly be neglected up to very high frequencies (e.g. 20 GHz and more). Our calculations show that the skin effect the substrate plays an important role in the transmission line

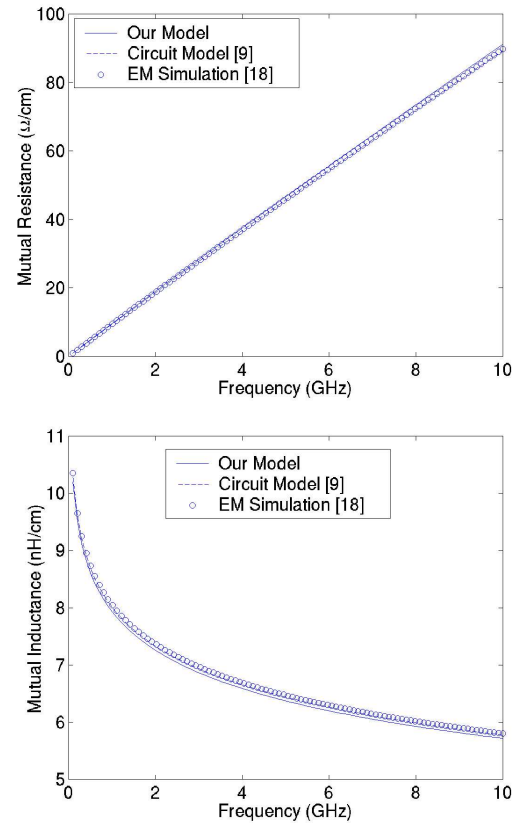


Figure 7. Mutual impedance parameters for symmetric coupled interconnects on low-resistivity silicon substrate. (a) Mutual resistance as a function of frequency, and (b) Mutual inductance as a function of frequency.

behavior, increasing the resistance per unit length of the lines (self resistance) from its dc value by approximately a factor of 2 at 10 GHz. Figs. 6 and 7 show the frequency-dependent impedance matrix parameters. The solid lines are computed by using our analytic model and the dashed lines and lines denoted by circles are the results from the quasi-magnetostatic analysis [9] and full-wave solutions [18]. The frequency response of proposed analytic model agrees well with these computed by the extracted equivalent-circuit model and full-wave simulator. The extracted equivalent-circuit model is based on the simultaneous discretization of interconnect conductors and silicon substrate, and takes into account the substrate skin effect, as well as the conductor skin and proximity effects. As expected, the lossy silicon substrate has more significant impact (substrate skin effect dominates) on the frequency-dependence of the impedance matrix parameters as compared to signal conductor effects (conductor skin effect can be neglected).

## 4 Conclusion

CAD-oriented analytical expressions have been proposed for the series impedance matrix parameters of symmetric coupled interconnects on conductive silicon substrate. The expressions holds for the lines whose metallizations have

very small cross sections, but larger than the skin penetration depth at operating frequency. In addition, the developed closed-form formulas describe the series impedance matrix parameter behavior over the whole frequency range (i.e. also in the transition region between dielectric quasi-TEM mode, skin-effect mode and slow-wave mode). Comparisons with numerical results concerning on-chip interconnects on highly conductive silicon substrate suggests that, for the small cross section of lines and in frequency range whereon the dc resistance model applies, the expressions for the series impedance matrix parameters presented are accurate enough and should be useful in the design of mixed-signal integrated circuits.

## Referências

- [1] H. Hasegawa, M. Furukawa, and H. Yanai, "Properties of microstrip line on Si-SiO<sub>2</sub> system," *IEEE Trans. Microwave Theory Tech.*, vol. MTT-19, pp. 869 - 881, 1971.
- [2] S. Zaage and E. Groteluschen, "Characterization of the broadband transmission behavior of interconnections on silicon substrate," *IEEE Trans. Comp., Hybrids, Manufact. Technol.*, Vol. 16, pp. 686 - 691, 1993.
- [3] V. Milanovic, M. Ozgur, D. C. DeGroot, J. A. Jargon, M. Gaitan, and M. E. Zaghoul, "Characterization of broad-band transmission for coplanar waveguides on CMOS silicon substrates," *IEEE Trans. Microwave Theory Tech.*, vol. MTT-46, pp. 632 - 640, 1998
- [4] D. F. Williams, "Metal-insulator-semiconductor transmission lines," *IEEE Trans. Microwave Theory Tech.*, vol. MTT-47, pp. 176 - 181, 1999.
- [5] T. Shibata and E. Sano, "Characterization of MIS structure coplanar transmission lines for investigation of signal propagation in integrated circuits," *IEEE Trans. Microwave Theory Tech.*, vol. MTT-38, pp. 881 - 890, 1990.
- [6] E. Groteluschen, L. S. Dutta, and S. Zaage, "Full-wave analysis and analytical formulas for the line parameters of transmission lines on semiconductor substrates," *Integration, The VLSI J.*, vol. 16, pp. 33 - 58, 1993.
- [7] J.-K. Wee, Y. - J. Park, H. - S. Min, D. - H. Cho, M. - H. Seung, and H. - S. Park, "Modeling the substrate effect in interconnect line characteristics of high speed VLSI circuits," *IEEE Trans. Microwave Theory Tech.*, vol. MTT-46, pp. 1436 - 1443, 1998.
- [8] J. Zheng, Y. C. Hahm, V. K. Tripathi, and A. Weisshaar, "CAD-oriented equivalent circuit modeling of on-chip interconnects on lossy silicon substrate," *IEEE Trans. Microwave Theory Tech.*, vol. MTT-48, pp. 1443 - 1451, 2000.
- [9] J. Zheng, V. K. Tripathi, and A. Weisshaar, "Characterization and modeling of multiple coupled on-chip interconnects on silicon substrate," *IEEE Trans. Microwave Theory Tech.*, vol. MTT-49, pp. 1733 - 1739, 2001.
- [10] M. Kamon, M. J. Tsuk, and J. K. White, "FASTHENRY: A multipole-accelerated 3-D inductance extraction program," *IEEE Trans. Microwave Theory Tech.*, vol. MTT-42, pp. 1750 - 1758, 1994.
- [11] H. Ymeri, B. Nauwelaers, K. Maex, D. De Roest, and M. Stucchi, "Analytic model for self and mutual frequency-dependent impedance of multiconductor interconnects on lossy silicon substrate," in *34th International Symposium on Microelectronics*, Baltimore, Maryland, October 8 - 11, 2001.
- [12] H. Ymeri, B. Nauwelaers, K. Maex, S. Vandenberghe, D. De Roest, and M. Stucchi, "New frequency-dependent formulas for mutual resistance and inductance of interconnects on lossy silicon substrate," in *European Gallium Arsenide and Other Semiconductors Application Symposium*, London, United Kingdom, September 24 - 27, 2001.
- [13] H. Ymeri, B. Nauwelaers, and K. Maex, "Simple and accurate expressions for distributed mutual inductance and resistance of semiconducting interconnects," *Appl. Phys. Letters*, vol. 79, pp. 388 - 391, 2001.
- [14] H. Ymeri, B. Nauwelaers, and K. Maex, "Distributed inductance and resistance per unit length formulas for VLSI interconnects on silicon substrate," *Microwave Opt. Techn. Letters*, vol. 30, pp. 302 - 304, 2001.
- [15] . A. Deutsch, G. V. Kopcsay, C. W. Surovic, B. J. Rubin, L. M. Terman, R. P. Dunne, T. A. Gallo and R. H. Denard, "Modeling and characterization of long on-chip interconnections for high-performance microprocessors," *IBM J. Res. Develop.*, vol. 39, pp. 547 - 567, May, 1995.
- [16] M. Kobayashi, "Longitudinal and transverse current distributions on microstrip and their closed-form expression," *IEEE Trans. Microwave Theory Tech.*, vol. MTT-33, pp. 784 - 788, Sept., 1985.
- [17] E. D. Sunde, *Earth Conduction Effects in Transmission Systems*, New York: Dover, 1968.
- [18] *Full-wave planar EM field solver Agilent Momentum*, Agilent EEs of EDA, Santa Rosa, CA.